energies

MDPI

Article

Research on Fault-Tolerant Operation Strategy of Permanent Magnet Synchronous Motor with Common DC Bus Open Winding Phase-Breaking Fault

Kangfei Lv [1,2], Xinwei Dong [1,*] and Cong Zhu [1]

[1] School of Electrical Engineering, China University of Mining and Technology, Xuzhou 221008, China; lkf@hytc.edu.cn (K.L.); zhu_cong0212@163.com (C.Z.)
[2] School of Physics and Electrical and Electronic Engineering, Huai Yin Normal University, Huaian 223300, China
* Correspondence: dxw_zju@163.com; Tel.: +86-17851568713

Abstract: In some key areas, fault-tolerant control is usually needed in order to enable the motor to operate continuously in fault mode. Given that it is difficult to detect the zero-sequence current of the open winding permanent magnet synchronous motor after the phase break fault occurs, the traditional zero-sequence current suppression strategy is no longer applicable after the phase break fault occurs. Therefore, a zero-sequence current suppression strategy for a common DC bus under a phase break fault is proposed in this paper. By establishing the mathematical model between the current component in the synchronous coordinate system and the current component and the zero-sequence current in the static coordinate system, the relationship between the non-fault phase current and the zero-sequence current in the open phase fault is analyzed. A method of suppressing the zero-sequence current by using proportional integral double resonance in a zero-sequence current control loop is proposed. In addition, according to the large number of calculations in traditional space vector modulation (SVPWM)—such as sector judgment and coordinate transformation—a decoupling modulation algorithm is proposed to modulate the reference voltage vector. Finally, the experimental platform for the common DC bus open winding permanent magnet synchronous motor is built, and the zero-sequence current suppression method for the common DC bus OW-PMSM under phase break fault is verified experimentally.

Keywords: open winding permanent magnet synchronous motor; phase break fault; zero-sequence current; decoupled modulation; fault-tolerant control

Citation: Lv, K.; Dong, X.; Zhu, C. Research on Fault-Tolerant Operation Strategy of Permanent Magnet Synchronous Motor with Common DC Bus Open Winding Phase-Breaking Fault. *Energies* **2022**, *15*, 2927. https://doi.org/10.3390/en15082927

Academic Editors: Rui Esteves Araújo and Elhoussin Elbouchikhi

Received: 27 January 2022
Accepted: 13 April 2022
Published: 15 April 2022

1. Introduction

A permanent magnet synchronous motor (PMSM) is widely used in industrial, transportation, military, and other important fields because of its simple and reliable structure, high power density, and high control precision [1,2]. In the traditional PMSM system, the motor is supplied by a single inverter, but due to the voltage withstand levels from switching devices, the application of PMSM in high-power situations is limited. For this reason, the relevant scholars put forward the idea of applying the open winding structure to the PMSM, that is, by opening the neutral point of the stator winding of the traditional PMSM and connecting it to an additional inverter, the motor can be supplied by two inverters at the same time [3]—which is called an open winding permanent magnet synchronous motor (Open-Winding PMSM, OW-PMSM). Therefore, under the same power level of switching devices, the rated power of an OW-PMSM can be doubled [4]. In addition, the power supply of two inverters makes the OW-PMSM system exhibit multilevel modulation characteristics [5] and has a strong fault-tolerant operation ability [6,7].

According to whether the inverter on both sides of the motor in the OW-PMSM system uses the same voltage source for a power supply, it can be divided into a common DC bus

system [8] and an isolated bus system [5]. The two structures are shown in Figure 1a,b, respectively. Compared with the isolation bus system shown in Figure 1a, the common DC bus system in Figure 1b needs only one voltage source, which can effectively reduce the cost and volume of the system. However, there is a zero-sequence current (Zero-Sequence Current, ZSC) in this system, which will cause torque ripple and additional loss [9] and will affect the performance of the OW-PMSM system. Therefore, the suppression of ZSC has become a hot topic in the common DC bus OW-PMSM system. For example, [10] proposed a method to generate a zero-axis reference voltage vector by flexibly adjusting the action time of the zero-voltage vector to suppress ZSC. Considering the influence of dead time setting on ZSC, a ZSC suppression strategy based on an allocation factor adjustment is proposed in [11,12] A control strategy of using an effective reference voltage vector to regulate zero-sequence reference voltage is proposed, which achieves the goal of suppressing ZSC with low switching times.

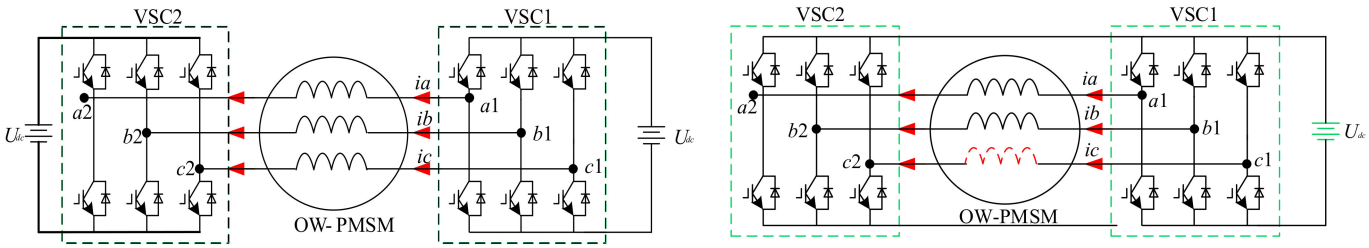

(**a**) (**b**)

Figure 1. Topology of OW-PMSM system. (**a**) The isolation bus system; (**b**) The common DC bus system.

When there is a phase-breaking fault in the traditional PMSM structure, its structure must be improved in order to achieve fault-tolerant operation. For example, in order to realize the operation of the PMSM phase break, [13] proposed a method to connect the neutral point of PMSM winding to the midpoint of the DC bus. In contrast, in the OW-PMSM system, due to the independent power supply of each phase winding, the system has a strong fault-tolerant ability, and the fault-tolerant operation can be realized only by relying on the remaining normal phase windings without changing the system structure [14]. However, there is still ZSC in the OW-PMSM system at this time, and because of the uncertainty of the current phase in the remaining two-phase windings, the ZSC component cannot be accurately obtained and the ZSC cannot be controlled in the closed loop, so the existing ZSC suppression side strategy [11,13] cannot be applied. The fault-tolerant control of OW-PMSM under open phase fault has been studied in [15,16]. Its fault-tolerant control strategy depends on the accurate mathematical model, the parameters of OW-PMSM, and the need for a large number of calculations. Therefore, this paper proposes a new open-phase fault-tolerant method for the OW-PMSM. This method does not need to change the hardware structure for current detection, and only needs to adjust the zero-sequence reference current according to the fault detection results to realize the zero-sequence current suppression. By calculating the zero-sequence reference current required in the state of open phase fault, the unnecessary zero-sequence current is suppressed by PIDR control. This method can be applied to the PMSM control system no matter if $i_d = 0$ control mode or $i_d \neq 0$ control mode is employed. The method of PWM is also very important from the computation complexity point of view. Therefore, a decoupling modulation algorithm in the fault state is proposed, which avoids the complex calculation processes, such as sector judgment and time calculation in SVPWM.

In the normal state of the OW-PMSM system, the ZSC can be obtained by averaging the current of the three-phase stator windings. However, this method of obtaining ZSC is no longer suitable for phase breaking faults of phase windings. Considering the phase relationship of the remaining two-phase current under the phase-breaking fault, this paper

establishes the mathematical model between the current component in the static coordinate system, the current component in the synchronous shafting and the ZSC, and deeply analyzes the relationship between the non-fault phase current and the ZSC in the case of a phase-breaking fault. Furthermore, the ZSC suppression scheme of the OW-PMSM system based on proportional integral double resonance (PIDR) control under a phase break fault is designed. In addition, in order to reduce the amount of computation in the control process, a zero-sequence current suppression strategy based on a three-phase decoupling modulation is proposed. Finally, the proposed ZSC suppression strategy for a common DC bus OW-PMSM system under phase failure is verified on the experimental platform.

2. Mathematical Model of Common DC Bus OW-PMSM System under Phase Break Fault

Taking the open circuit of *c*-phase winding shown in Figure 1 as an example, the mathematical model of the common DC bus OW-PMSM system under a phase breaking fault is analyzed. When the *c*-phase winding is broken, the OW-PMSM mathematical model can be expressed as follows:

$$\begin{aligned} \begin{bmatrix} u_a \\ u_b \end{bmatrix} &= \frac{d}{dt}\begin{bmatrix} \psi_a \\ \psi_b \end{bmatrix} + \begin{bmatrix} R_s & \\ & R_s \end{bmatrix}\begin{bmatrix} i_a \\ i_b \end{bmatrix} \\ &= U_{dc}\left(\begin{bmatrix} S_{a1} \\ S_{b1} \end{bmatrix} - \begin{bmatrix} S_{a2} \\ S_{b2} \end{bmatrix}\right) \end{aligned} \tag{1}$$

In the formula, u_x, i_x, and $\psi_x (x = a, b, c)$ represent the phase voltage, phase current, and flux of the x phase, respectively, while R represents the stator winding resistance, U_{dc} represents the DC bus voltage, and S_{x1} and S_{x2} represent the switching functions of inverter 1 and inverter 2, which satisfy the following corresponding relations:

$$S_x = \begin{cases} 0 \text{ The upper bridge arm is closed and the lower bridge arm is open} \\ 1 \text{ The upper bridge arm is opened and the lower bridge arm is closed} \end{cases} \tag{2}$$

Since the OW-PMSM with common DC bus has a zero-sequence circuit, the model of the OW-PMSM in the dq0 synchronous coordinate system, considering the third flux linkage of the permanent magnet, can be described as,

$$\begin{bmatrix} u_d \\ u_q \\ u_0 \end{bmatrix} = \begin{bmatrix} L_d di_d/dt + Ri_d - \omega L_q i_q \\ L_q di_q/dt + Ri_q + \omega L_d i_d + \omega\psi_f \\ L_0 di_0/dt + Ri_0 - 3\omega\psi_{3f}\sin(3\theta) \end{bmatrix} \tag{3}$$

$$\begin{cases} u_0 = \frac{1}{3}(u_a + u_b + u_c) \\ i_0 = \frac{1}{3}(i_a + i_b + i_c) \end{cases} \tag{4}$$

The zero-sequence equivalent circuit of the OW-PMSM system could be obtained as shown in Figure 2, in which u_{01} and u_{02} are generated by VSC 1 and VSC 2, respectively, and $3\omega\psi_{3f}\sin 3\theta$ is generated by the third back EMF.

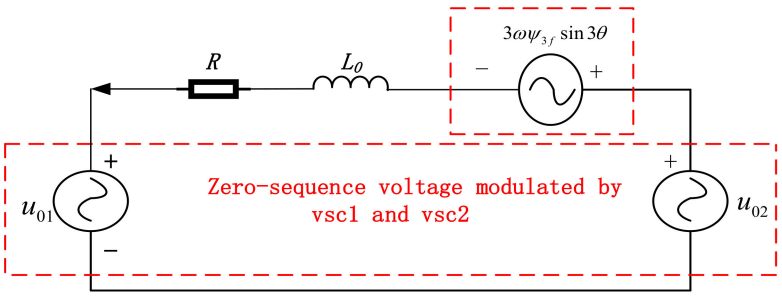

Figure 2. Zero-sequence equivalent circuit of OW-PMSM.

In the case of an open circuit of *c*-phase winding, the output voltage of the bridge arm corresponding to *c*-phase winding has nothing to do with S_{c1} and S_{c2}. Therefore, the number of output voltage vectors for inverter 1 and inverter 2 is reduced from 8 to 4, and the corresponding vector distribution is shown in Figure 3.

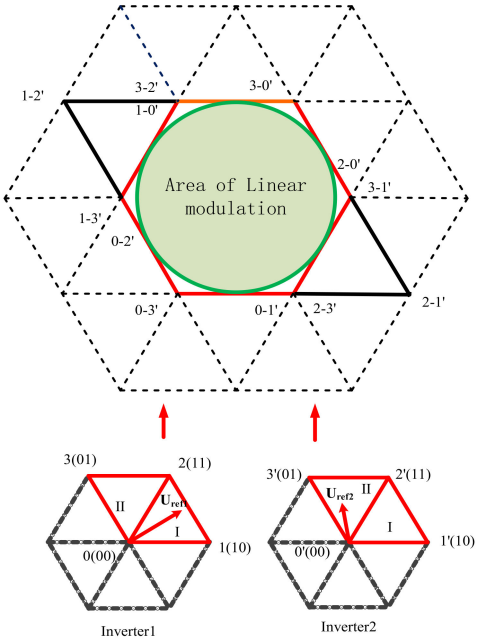

Figure 3. Distribution of the voltage vectors under the open-phase fault of c-phase.

According to the OW-PMSM mathematical model (1), the voltage vector distribution of the OW-PMSM system is shown in Figure 3, in which each voltage vector is expressed in the form of *m*-*n*′, and *m* and *n*′ are the output voltage vectors of inverter 1 and inverter 2, respectively. It can be seen from the figure that the open winding system can still provide a complete linear modulation range after the phase break fault, but the maximum linear modulation degree is reduced to half of the original—from $2\sqrt{3}U_{dc}/3$ to $\sqrt{3}U_{dc}/3$—indicating that the open winding permanent magnet synchronous motor can still operate in fault tolerance.

3. Zero-Sequence Current Suppression after Phase Break Fault

In the closed-loop control system of the open-winding permanent magnet synchronous motor (PMSM), when the open-phase fault occurs in the arbitrary phase, the current in this phase drops to zero accordingly. Therefore, in order to keep the motor torque unchanged after the fault, the two non-fault phase currents should produce the same d-q current as before the fault state. Take the *c*-phase open circuit as an example, i_c will drop to zero. Therefore, the reference currents of i_c^* should be set to zero. According to the inverse clark transformation (5), the zero-sequence reference current can be obtained as (6), where i_a^*, i_b^*, i_c^* are reference currents in the *a*-*b*-*c* Frame, and i_α^*, i_β^*, and i_0^* are reference currents in the $\alpha\beta$0-axis.

$$\begin{bmatrix} i_a^* \\ i_b^* \\ i_c^* \end{bmatrix} = \begin{bmatrix} 1 & 0 & 1 \\ -\frac{1}{2} & \frac{\sqrt{3}}{2} & 1 \\ -\frac{1}{2} & -\frac{\sqrt{3}}{2} & 1 \end{bmatrix} \begin{bmatrix} i_\alpha^* \\ i_\beta^* \\ i_0^* \end{bmatrix} \tag{5}$$

$$i_0^* = \frac{1}{2} i_\alpha^* + \frac{\sqrt{3}}{2} i_\beta^* \tag{6}$$

Furthermore, the post-fault reference current of phase a and phase b can be written as,

$$\begin{bmatrix} i_a^* \\ i_b^* \end{bmatrix} = \begin{bmatrix} \frac{3}{2} & \frac{\sqrt{3}}{2} \\ 0 & \sqrt{3} \end{bmatrix} \begin{bmatrix} i_\alpha^* \\ i_\beta^* \end{bmatrix} \tag{7}$$

$$\begin{bmatrix} i_\alpha^* \\ i_\beta^* \end{bmatrix} = \begin{bmatrix} \cos\theta & -\sin\theta \\ \sin\theta & \cos\theta \end{bmatrix} \begin{bmatrix} i_d^* \\ i_q^* \end{bmatrix} \tag{8}$$

According to the inverse Park transformation (8), where i_d^* and i_q^* are the reference currents in the dq-axis, the reference healthy current i_a^* and i_b^* can be written as,

$$\begin{aligned} i_a^* &= \sqrt{3}(\tfrac{1}{2}\cos\theta - \tfrac{\sqrt{3}}{2}\sin\theta)i_q^* + \sqrt{3}(\tfrac{\sqrt{3}}{2}\cos\theta + \tfrac{1}{2}\sin\theta)i_d^* \\ &= \sqrt{3}(\cos\tfrac{\pi}{3}\cos\theta - \sin\tfrac{\pi}{3}\sin\theta)i_q^* + \sqrt{3}(\sin\tfrac{\pi}{3}\cos\theta + \cos\tfrac{\pi}{3}\sin\theta)i_d^* \\ &= \sqrt{3}\cos(\theta + \tfrac{\pi}{3})i_q^* + \sqrt{3}\sin(\theta + \tfrac{\pi}{3})i_d^* \end{aligned} \tag{9}$$

$$i_b^* = \sqrt{3}(i_q^*\cos\theta + i_d^*\sin\theta) \tag{10}$$

Expressed in the form of a matrix, which is:

$$\begin{bmatrix} i_a^* \\ i_b^* \end{bmatrix} = \sqrt{3}\begin{bmatrix} \cos(\theta + \frac{\pi}{3}) & \sin(\theta + \frac{\pi}{3}) \\ \cos\theta & \sin\theta \end{bmatrix} \begin{bmatrix} i_q^* \\ i_d^* \end{bmatrix} \tag{11}$$

According to the definition of a zero-sequence current, the zero-sequence reference current is:

$$i_0^* = \frac{1}{3}(i_a^* + i_b^* + i_c^*) \tag{12}$$

In the case of non-fault, the three-phase current is symmetrically distributed at 120 degrees, so i_0^* is 0.

In the case of phase c disconnection:

$$i_0^* = 3i_q^*\cos(\theta + \pi/6) + 3i_d^*\sin(\theta + \pi/6) \tag{13}$$

In the case of an open phase fault, the zero-sequence current i_0^* is the fundamental current necessary to maintain the normal operation of the motor. According to Formulas (11) and (13), the vector diagram of the c-phase open circuit can be drawn, as shown in Figure 4c. Similarly, the vector distribution of phase a and phase b in the case of an open circuit can be obtained as shown in Figure 4a,b, where the dotted line of i_{a-pre}^*, i_{b-pre}^*, i_{c-pre}^* are the reference currents for the pre-fault $i_a^*, i_b^*, i_c^*, i_0^*$ are the reference currents for the post-fault condition.

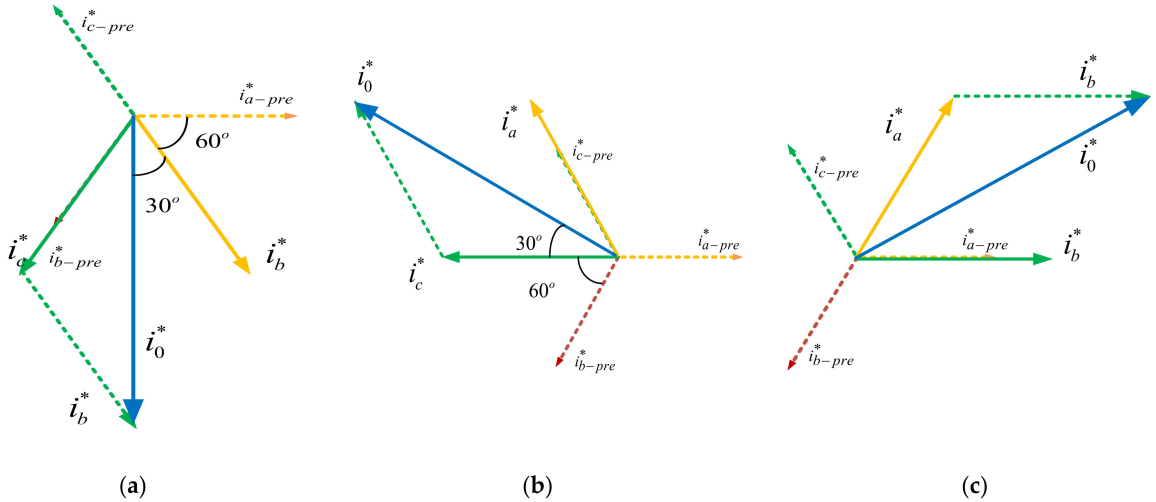

(**a**) (**b**) (**c**)

Figure 4. Non-fault phase reference current vector distribution in the case of fault. (**a**–**c**) Phase break.

From the above analysis, it can be seen that after the phase-breaking fault, the amplitude of the non-fault phase current is $\sqrt{3}$ times that of the pre-fault phase current, and the phase difference changes from 120 degrees to 60 degrees. According to the definition of a zero-sequence current, the fundamental zero-sequence current to maintain the normal operation of the system is $\left(i_a^* + i_b^*\right)/3$. In addition to the fundamental zero-sequence current, there is also the third harmonic current i_{03}^* formed by the back EMF of the permanent magnet. Therefore, the zero-sequence current control loop is composed of two parts, as shown in Figure 5: one is to track the zero-sequence fundamental reference current and the other is to suppress the third harmonic current.

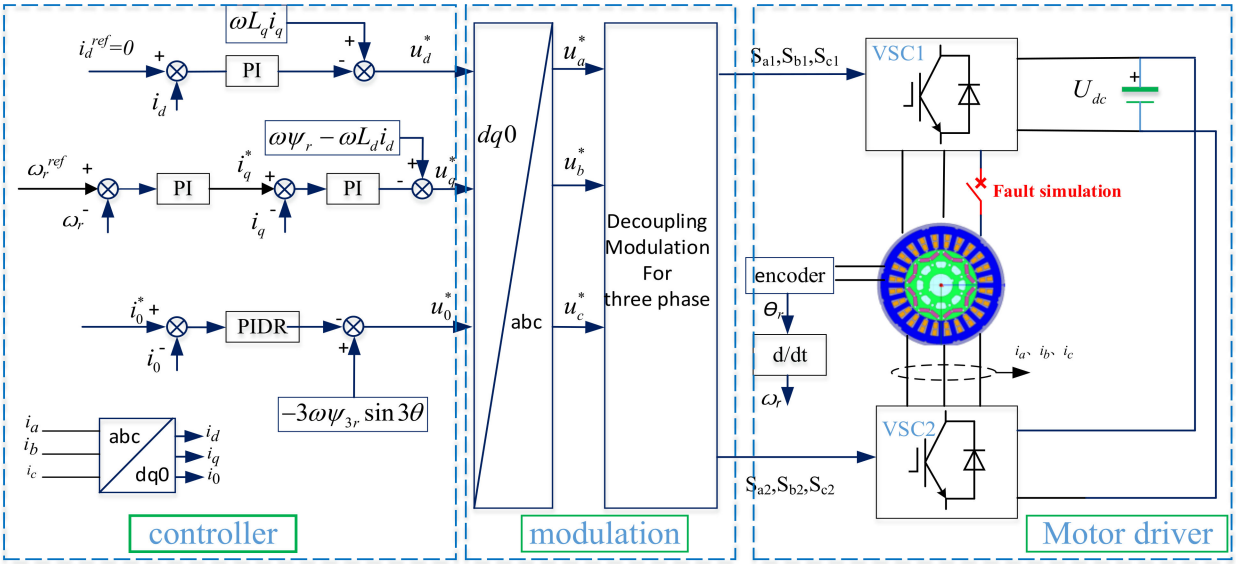

Figure 5. Zero-sequence current suppression method of common DC bus OW-PMSM based on PIDR under phase break fault.

In order to realize the tracking control of the fundamental and third harmonics, the zero-sequence current loop adopts a proportional integral double resonant control PIDR, and its transfer function is:

$$G_{PIDR} = k_{P3} + \frac{k_{i3}}{s} + \frac{k_{r1}\omega_{c1}s}{s^2 + 2\omega_{c1} + \omega_1^2} + \frac{k_{r2}\omega_{c2}s}{s^2 + 2\omega_{c2} + \omega_2^2} \tag{14}$$

K_{p3} is proportionality coefficient, K_{r1} is the integral coefficient, K_{r1} and K_{r2} are the resonance coefficients, ω_{c1} and ω_{c2} are the cut-off frequency, and ω_1, ω_2 are the resonance frequency.

The control goal of the resonant part is the fundamental wave and the third harmonic, so the resonance angular frequency is set to the fundamental angular frequency and the cubic harmonic angular frequency, respectively. For example, when the fundamental frequency is 50 HZ, set ω_{c1} and ω_{c2} to 50 πrad/s and 150 πrad/s. When the switching frequency of PWM modulation is high, such as (10 k), the influence of digital delay caused by the discretization of a continuous system on the control system can be ignored. If the switching frequency is reduced, such as 1 K or less, delay compensation should be added to the transfer function of the control system. The PIDR and PI parameters in Figure 5 need to be reset. After resetting, the system can still operate stably, but it will cause problems such as increased waveform harmonic distortion, reduced control system bandwidth, and reduced speed regulation performance. From the perspective of universality, the parameters of PIDR are set according to the switching frequency 10 K [17], where K_{p3} and K_{i3} are both 10 and K_{r1} and K_{r2} are 100, respectively. The corresponding Bode diagram is shown in Figure 6.

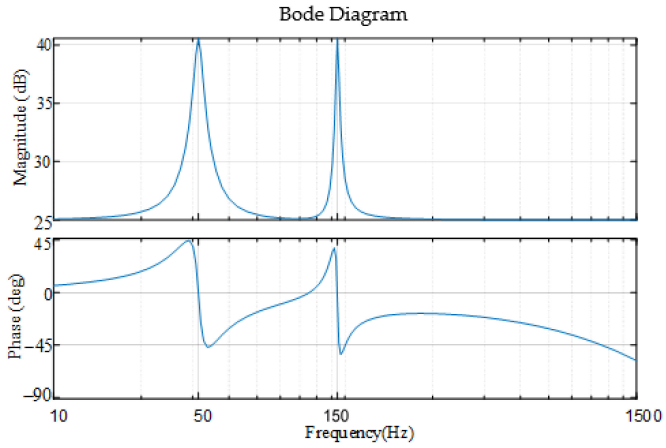

Figure 6. PIDR Bode Diagram when the fundamental frequency is 50 Hz.

It can be seen from Figure 6 that the amplitude of the fundamental wave and the third harmonic reaches the maximum 40.6 dB, which has a larger amplitude-frequency characteristic and can control the fundamental current and the third harmonic current in the zero-sequence current control circuit.

4. Three-Phase Decoupling Modulation

During the process of SVPWM vector modulation, it is necessary to judge the sector, which has a large amount of computation. In order to reduce the amount of calculation, a decoupling modulation algorithm is designed in this paper. The given voltage of the *dq0* three-axis is directly transformed into the given voltage of the non-fault phase and the decoupling modulation of the non-fault phase is realized in the *abc* coordinate system. Taking the *c*-phase fault as an example, the modulation process is introduced.

Given that the phases of the open winding permanent magnet synchronous motor are independent of each other, the non-fault phase can be modulated separately.

$$\begin{bmatrix} u_a^* \\ u_b^* \end{bmatrix} = U_{dc}\left(\begin{bmatrix} D_{a1} \\ D_{b1} \end{bmatrix} - \begin{bmatrix} D_{a2} \\ D_{b2} \end{bmatrix}\right) \tag{15}$$

Can be obtained according to the voltage reference instruction:

$$\begin{bmatrix} u_a^*/u_{dc} \\ u_b^*/u_{dc} \end{bmatrix} = \begin{bmatrix} D_{a1} - D_{a2} \\ D_{b1} - D_{b2} \end{bmatrix} \tag{16}$$

To determine D_{m1} and D_{m2}, $m = a, b$. A qualification, $D_{m1} + D_{m2} = 1$, also needs to be added so that it can be uniquely determined.

$$\begin{cases} D_{a1} + D_{a2} = 1 \\ D_{b1} + D_{b2} = 1 \end{cases} \tag{17}$$

The duty cycle of the VSC1 and VSC2 non-fault phase can be uniquely determined.

$$\begin{cases} D_{x1} = \frac{1}{2}(1 + \frac{u_x^*}{u_{dc}}) \\ D_{x2} = \frac{1}{2}(1 - \frac{u_x^*}{u_{dc}}) \end{cases} \tag{18}$$

x is the non-faulty phase in a, b, c.

According to the duty cycle and PWM cycle, the driving signal (S_{x1}, S_{x2}, S_{x3}) of each arm switch can be calculated. Taking $u_a^* = 0.8U_{dc}$, $u_b^* = -0.1U_{dc}$ as an example, we can get $D_{a1} = \frac{1}{2}(1 + 0.8) = 0.9$, $D_{a2} = \frac{1}{2}(1 - 0.8) = 0.1$, $D_{b1} = \frac{1}{2}(1 - 0.1) = 0.45$, and $D_{b2} = \frac{1}{2}(1 + 0.1) = 0.55$. Therefore, the modulated pulse sequence can be obtained as shown in Figure 7.

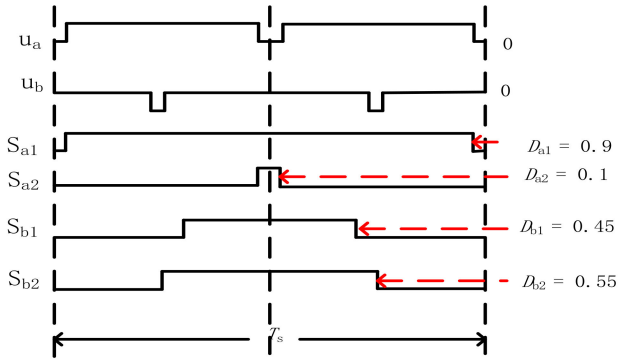

Figure 7. Modulation sequence.

After the single-phase open-circuit fault occurs, the linear modulation interval of the non-fault phase $u_x^* u$ is

$$-\frac{1}{\sqrt{3}}u_{dc} \le u_x^* \le \frac{1}{\sqrt{3}}u_{dc} \tag{19}$$

With the increase in speed, the problem of overmodulation will occur when the value range of u_x^* does not meet Formula (19). At this point, the following strategies can be used to adjust:

$$\begin{cases} u_{\max} = \max(u_m, u_n) \\ u_{\min} = \min(u_m, u_n) \end{cases} \tag{20}$$

Define the adjustment variable as Δu

$$\Delta u = \begin{cases} u_{dc}/\sqrt{3} - u_{\max}(u_{\max} > u_{dc}/\sqrt{3}) \\ -u_{dc}/\sqrt{3} - u_{\min}(u_{\min} < -u_{dc}/\sqrt{3}) \end{cases} \quad u_{x'}^* = u_x^* + \Delta u \tag{21}$$

$u_{x'}^*$ is the adjusted reference voltage.

After the phase-breaking fault occurs, we should first ensure that the motor maintains operation, and then consider the suppression of the zero-sequence current. The suppression ability of the zero-sequence current is affected by the reference voltage u_d^* and u_q^*. According to the above analysis, the modulation range of the zero-sequence reference voltage u_0^* is shown in Formula (22) and the available modulation range is shown in Figure 8.

$$-1 - m^* \min(\cos(\theta + \theta_u), \cos(\theta + \theta_u - \pi/3)) \le \frac{u_0}{u_{DC}} \le 1 - m^* \max(\cos(\theta + \theta_u), \cos(\theta + \theta_u - \pi/3)) \tag{22}$$

θ_u is the angle between the reference voltage u_{ref} and the d axis, $m^* = \frac{u_{ref}}{u_{dc}}$, $0 \le m^* \le 1/\sqrt{3}$.

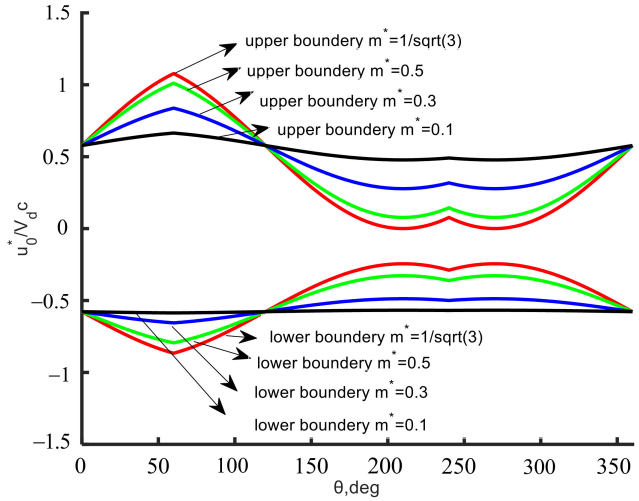

Figure 8. Available modulation range for u_0^*.

5. Experiment Verification

In order to verify the effectiveness of the control strategy of the common DC bus OW-PMSM system proposed in this paper, an OW-PMSM test system is built for testing, as shown in Figure 9. Both ends of the state windings are connected to an inverter whose DC buses are connected to DC power. An AC synchronous motor controlled by an ABB converter is used as a load. An increment type photoelectric encoder is mounted on the shaft of the OW-PMSM. The speed information is sent into the control board. The control signal of the inverters is provided by the control board embedded with a TMS320F28377 processor. The inverter and motor specifications are shown in Table 1. The switching frequency and sampling period frequency are set to 10 kHz, and the bus voltage is 200 V.

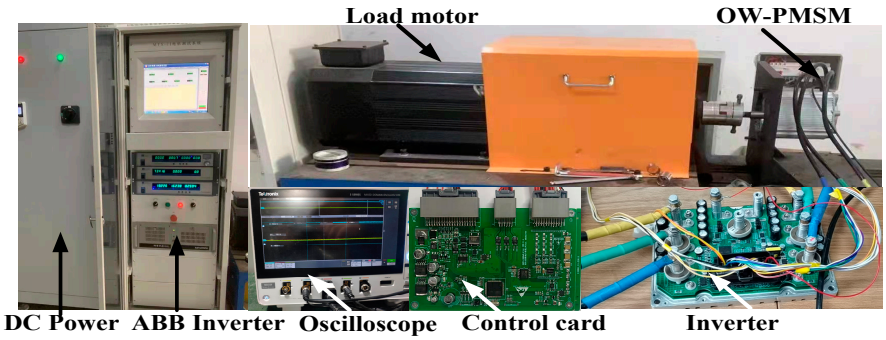

Figure 9. Experimental platform.

Table 1. OW-PMSM parameters.

Parameters	Numerical Value
d-axis inductor/mH	37
q-axis inductor/mH	71
Permanent magnet flux linkage/Wb	0.553
Rated frequency/Hz	50
Rated speed/(r/min)	1000
Rated load/N·m	5
Stator resistance/Ω	3.9
Pole pair	3

First of all, under the experimental condition of the rated load of 5 N·m and rotational speed of 500 r/min, the effect of the control strategy proposed in this paper is tested when the OW-PMSM changes from the normal state to the phase-breaking state, and the test results are shown in Figures 10 and 11.

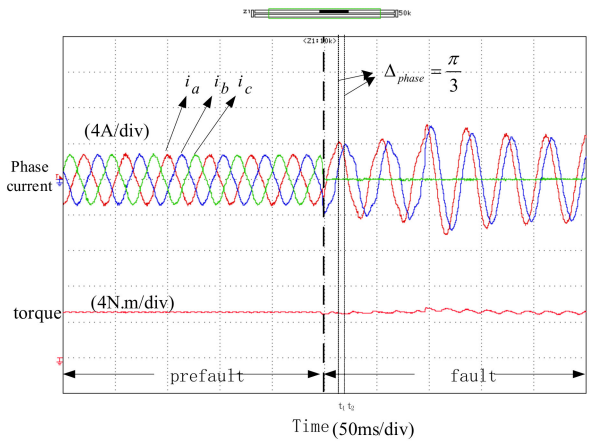

Figure 10. The dynamic comparison before and after the open-phase fault.

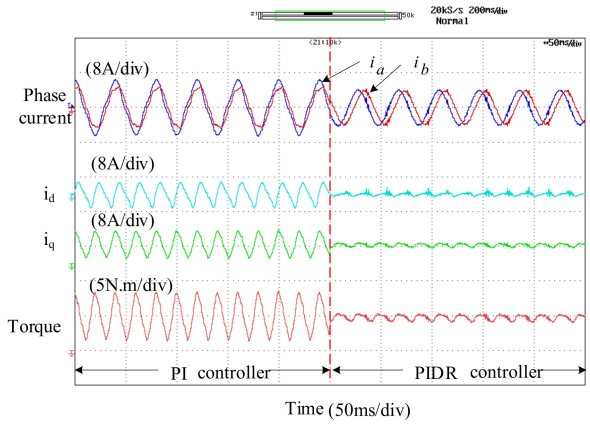

Figure 11. The experimental comparison before and after the application of the proposed PIDR controller.

From the comparison of the waveforms before and after the phase break in Figure 9, it can be seen that after the winding is broken, the amplitude of the phase current increases from 2.8 A to 4.8 A, which is magnified by 1.71 times, and the phase difference of the non-fault phase is 60 degrees. Which is consistent with the above theoretical analysis, and the fluctuation of the torque increases from ±0.12.m to ±0.44 N·m.

Then, under the same test conditions, the effect of the PIDR controller proposed in this paper for suppressing ZSC is tested. The experimental results are shown in Figure 12.

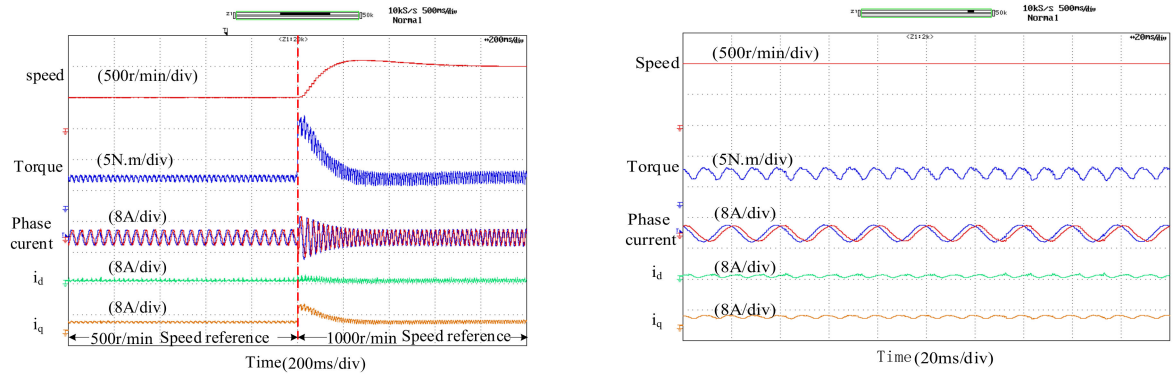

(**a**) (**b**)

Figure 12. The dynamic performance of the proposed scheme. (**a**) Dynamic performance; (**b**) Enlarged view at 1000 r/min.

It can be seen from Figure 12 that after using the PIDR controller proposed in this paper, the fluctuation of the *d*-axis current and *q*-axis current is reduced from ±3.5 A to ±0.6 A. From the change of current harmonic components in Figure 13, it can be seen that the proposed control scheme can effectively suppress the third harmonic components in the zero-sequence circuit, and the torque ripple is well suppressed from ±3.2 N·m to ±0.5 N·m.

In order to verify the control effect of the proposed control strategy in the dynamic process, the load torque is set to 5 N·m and the speed reference instruction is set to step from 500 r/min to 1000 r/min. The experimental results are shown in Figure 12. It can be seen from the waveform that the speed of the motor completely follows the speed reference instruction after a short adjustment process of 0.6 s.

Figure 14 shows the pulse modulation sequence waveform under decoupling modulation. In any control period, the duty cycle sum of the upper bridge arm at both ends of the winding is 1, which is equivalent to a svpwm vector modulation. The experimental results are consistent with the theoretical analysis.

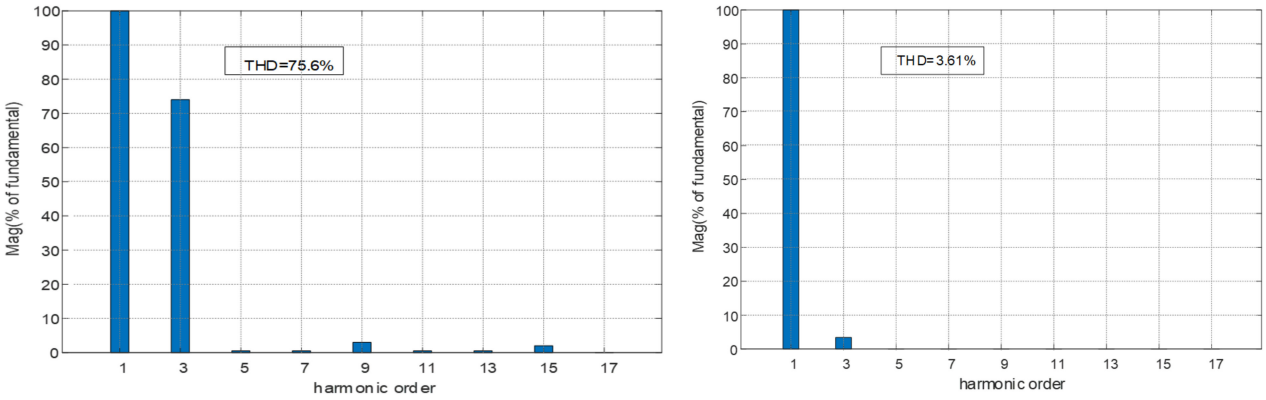

(**a**) (**b**)

Figure 13. FFT analyses of a phase current. (**a**) Without zero suppression; (**b**) Adopt zero suppression.

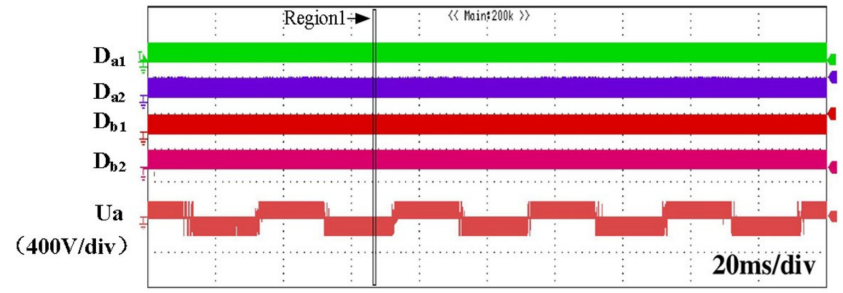

(**A**)

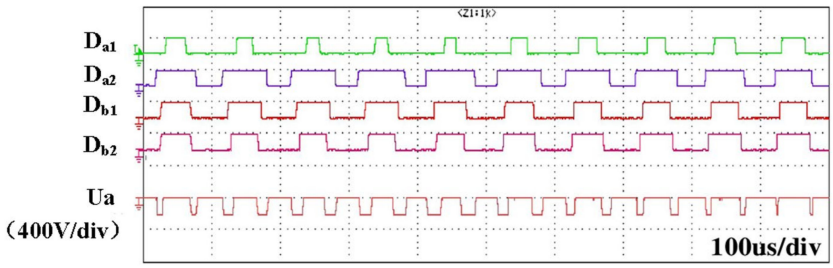

(**B**)

Figure 14. Experimental test of the proposed method. (**A**) The modulation sequence based on decoupling modulation; (**B**) Enlarge view of Region1.

6. Conclusions

In this paper, a ZSC suppression control strategy for a common DC bus OW-PMSM system under phase winding open fault based on decoupling modulation is proposed. The following conclusions can be drawn:

1. Under phase open fault, because the original three-phase current balance is broken, the ZSC is no longer zero, so the zero-sequence reference current needs to be recalculated. This paper analyzes the characteristics of the zero-sequence current before and after the fault and solves the problem of difficult extraction of the third harmonic current after the fault by recalculating the reference of the ZSC in fore-and-aft operation, which is conducive to the post-fault closed-loop control of the ZSC.
2. According to the vector distribution relationship between the non-fault phase current and the zero-sequence current, a ZSC suppression scheme based on PIDR control is designed, which can track and control the zero-sequence fundamental current and the third harmonic current in the zero-sequence current control circuit and realize the suppression of ZSC.

3. According to the characteristics of voltage modulation in the OW-PMSM system under phase break fault, a modulation method based on three-phase decoupling is proposed, which can generate a modulation pulse sequence directly according to the reference voltage, thus simplifying the complexity of modulation in common DC bus OW-PMSM systems under phase break faults.

Author Contributions: Conceptualization, K.L. and X.D.; Data curation, K.L. and C.Z.; Methodology, K.L.; Project administration, X.D.; Resources, X.D.; Software, K.L.; Supervision, X.D.; Validation, C.Z.; Visualization, C.Z.; Writing—original draft, K.L. All authors have read and agreed to the published version of the manuscript.

Funding: This research received no external funding.

Institutional Review Board Statement: Not applicable.

Informed Consent Statement: Not applicable.

Data Availability Statement: The study did not report any data.

Conflicts of Interest: The authors declare no conflict of interest.

References

1. Mendoza-Mondragón, F.; Hernandez-Guzmán, V.M.; Rodríguez-Reséndiz, J. Robust speed control of permanent magnet synchronous motors using two-degrees-of-freedom control. *IEEE Trans.* **2018**, *65*, 6099–6108. [CrossRef]
2. Jilong, L.; Fei, X.; Yang, S. Position-Sensorless Control Technology of Permanent-Magnet Synchronous Motor-a Review. *Trans. China Electrotech. Soc.* **2017**, *32*, 77–88.
3. Song, Z.; Ma, X.; Yu, Y. Design of zero-sequence current controller for open-end winding PMSMs considering current measurement errors. *IEEE Trans. Power Electron.* **2020**, *35*, 6127–6139. [CrossRef]
4. Byen, B.; Baek, S.; Cho, Y.; Choe, G. Dual SRF based torque ripple mitigation strategy for a fault tolerant PMSM drive system. In Proceedings of the 2015 9th International Conference on Power Electronics and ECCE Asia (ICPE-ECCE Asia), Seoul, Korea, 1–5 June 2015; IEEE: Piscataway, NJ, USA, 2015; pp. 1724–1729.
5. Reddy, B.V.; Somasekhar, V.T.; Kalya, Y. Decoupled Space-V ector PWM Strategies for a Four-Level Asymmetrical Open-End Winding Induction Motor Drive with Waveform Symmetries. *IEEE Trans.* **2011**, *58*, 5130–5141.
6. Nian, H.; Yijie, Z.; Hengli, Z. Fault-Tolerant Control Technique of Permanent Magnet Synchronous Generator Based on Open Winding Configuration. *Trans. China Electrotech. Soc.* **2015**, *30*, 58–67.
7. Nguyen, N.K.; Meinguet, F.; Semail, E.; Kestelyn, X. Fault-Tolerant Operation of an Open-End Winding Five-Phase PMSM Drive with Short-Circuit Inverter Fault. *IEEE Trans.* **2016**, *63*, 595–605. [CrossRef]
8. Cha, H.; Vu, T.; Kim, J. Design and control of proportional-resonant controller based photovoltaic power conditioning system. In Proceedings of the 2009 IEEE Energy Conversion Congress and Exposition, San Jose, CA, USA, 20–24 September 2009; IEEE: Piscataway, NJ, USA, 2009; pp. 2198–2205.
9. Hu, W.; Nian, H.; Zheng, T. Torque Ripple Suppression Method with Reduced Switching Frequency for Open-Winding PMSM Drives with Common DC Bus. *IEEE Trans. Ind. Electron.* **2019**, *66*, 674–684. [CrossRef]
10. Zhou, Y.; Nian, H. Zero-Sequence Current Suppression Strategy of Open-Winding PMSG System with Common DC Bus Based on Zero Vector Redistribution. *IEEE Trans. Ind. Electron.* **2015**, *62*, 3399–3408. [CrossRef]
11. An, Q.; Liu, J.; Peng, Z.; Sun, L.; Sun, L. Dual-Space Vector Control of Open-End Winding Permanent Magnet Synchronous Motor Drive Fed by Dual Inverter. *IEEE Trans. Power Electron.* **2016**, *31*, 8329–8342. [CrossRef]
12. Hu, W.; Nian, H.; Sun, D. Zero-Sequence Current Suppression Strategy with Reduced Switching Frequency for Open-End Winding PMSM Drives with Common DC BUS. *IEEE Trans. Ind. Electron.* **2019**, *66*, 7613–7623. [CrossRef]
13. Gajanayake, C.J.; Bhangu, B.; Nadarajan, S.; Jayasinghe, G. Fault tolerant control method to improve the torque and speed response in PMSM drive with winding faults. In Proceedings of the IEEE 9th International Conf on Power Electron and Drive Systems, Singapore, 5–8 December 2011; IEEE: Piscataway, NJ, USA, 2011; pp. 956–961.
14. Ruan, C.; Hu, W.; Nian, H.; Sun, D. Open-Phase Fault Control in Open-Winding PMSM System with Common DC Bus. In Proceedings of the 2019 IEEE Applied Power Electronics Conference and Exposition (APEC), Anaheim, CA, USA, 17–21 March 2019; IEEE: Piscataway, NJ, USA, 2019; pp. 1052–1056.
15. Song, Z.F.; Zhou, F.J.; Yu, Y.; Zhang, R.; Hu, S.Y. Open-Phase Fault-Tolerant Predictive Control Strategy for Open-End-Winding Permanent Magnet Synchronous Machines Without Post Fault Controller Reconfiguration. *IEEE Trans. Ind. Electron.* **2021**, *68*, 3770–3781. [CrossRef]
16. Béthoux, O.; Labouré, E.; Remy, G.; Berthelot, E. Real-Time Optimal Control of a 3-Phase PMSM in 2-Phase Degraded Mode. *IEEE Trans. Veh. Technol.* **2017**, *66*, 2044–2052. [CrossRef]
17. Tang, C.; Liang, K.; Shu, Z.Y.; He, Q.Q.; Chen, Q.H. Analysis and Design of Multiple Resonant Current Control for Grid-Connected Converters. *IEEE J. Emerg. Sel. Top. Power Electron.* **2022**, *10*, 2539–2546. [CrossRef]